Electronic supplementary information

The key effect of polymorphism during Pb^{II} uptake by calcite and aragonite.

Fulvio Di Lorenzo[1*], Cristina Ruiz-Agudo[2] and Sergey V. Churakov[1,3]

1) Institute of Geological Sciences, University of Bern, Bern 3012, Switzerland;

2) Department of Physical Chemistry, University of Konstanz, Konstanz 78457, Germany;

3) Laboratory for Waste Management, Paul Scherrer Institut, Villigen 5232, Switzerland.

* Corresponding author. Email: fulvio.dilorenzo@geo.unibe.ch; Tel: +41 316318770.

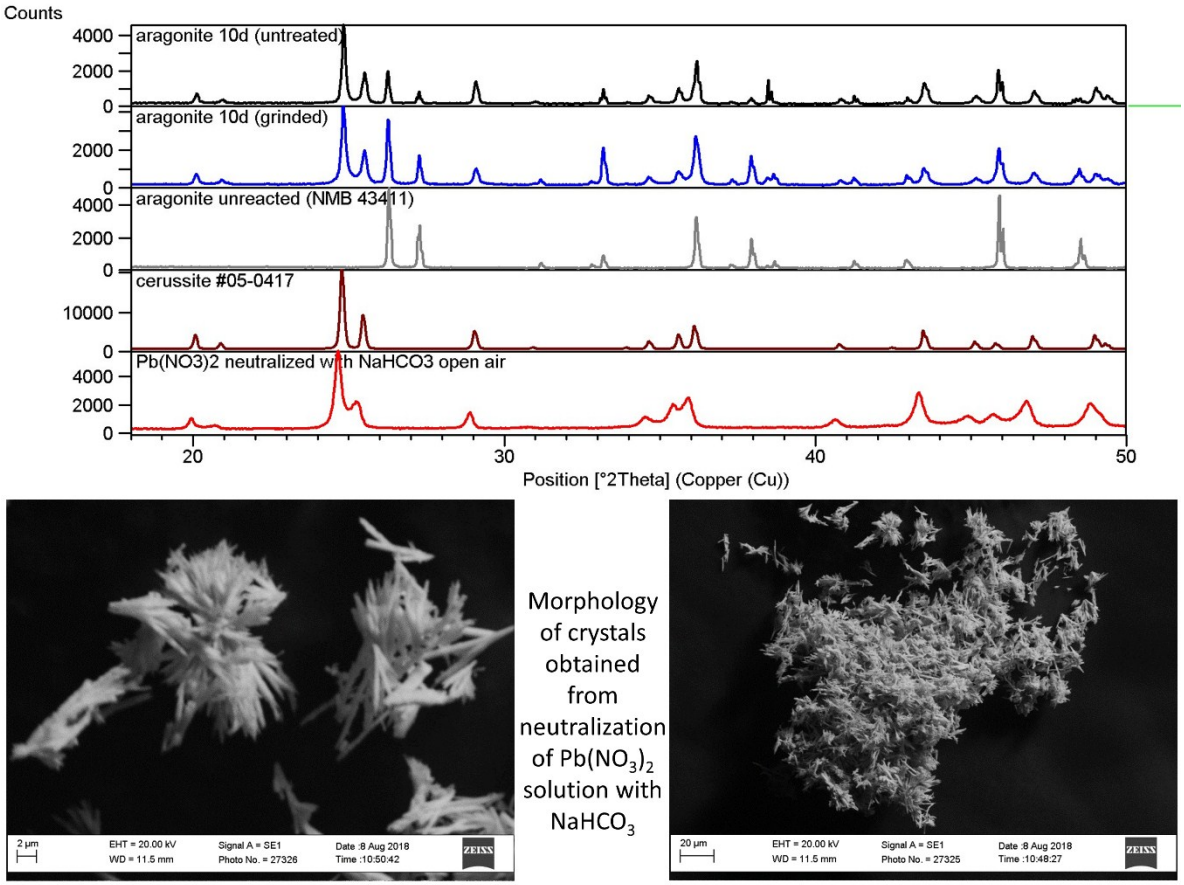

Figure S1. Diffractograms of aragonite sample before and after the interaction with $Pb(NO_3)_2$ solutions. In particular, we reported the diffractograms of the same sample collected after 10 days of interaction without any treatment (labeled: untreated) and after grinding (grinded); this comparison clearly shows the high shielding effect exerted by the layer of cerussite overgrown onto aragonite crystals. In the bottom part of the figure we reported two SEM images (secondary electron) of the solid formed due to the addition of $NaHCO_3$ to a $Pb(NO_3)_2$ solution. The XRD pattern of this sample clearly identify it as cerussite and the morphology is very similar to the elongated crystals that constitute the main precipitate during the AFM in situ experiments.

Figure S2. Mosaic picture (6x3 mm) of the epoxy mount of the sections of aragonite crystals after 10 days of interaction with the $Pb(NO_3)_2$ solution. The high definition of the image allows to see that every aragonite crystal is completely surrounded by a layer of cerussite demonstrating the efficiency of the passivation driven by the crystallographic control.

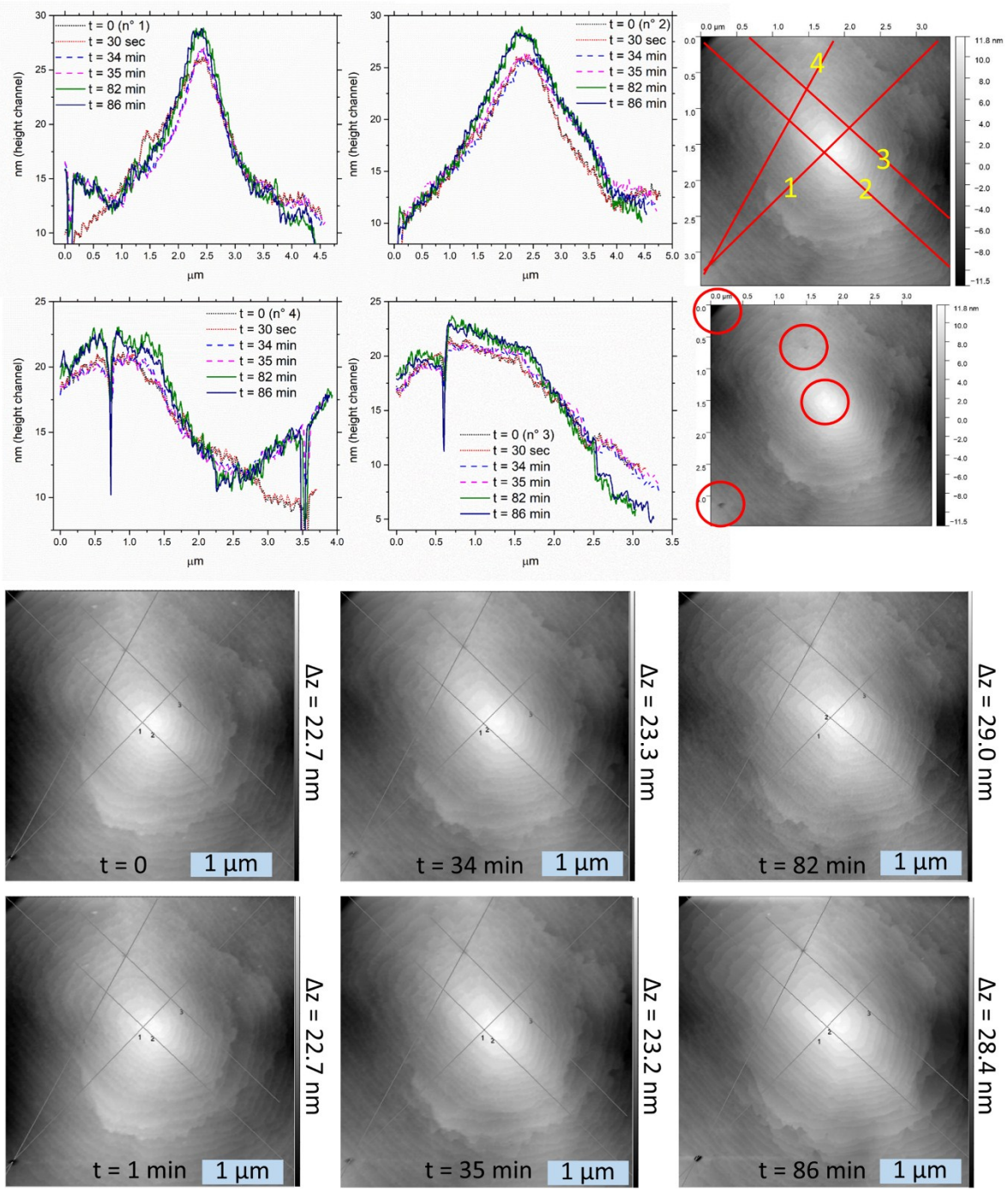

Figure S3. Accurate profile measurements of the hillock observed in situ during the growth of a Pb-bearing carbonate phase with hexagonal morphology (hydrocerussite). The evolution of the sections with time is reported for 4 sections. They were specifically drawn to correct the measurements for the drift of the image taking advantage of 4 points easy to identify (red circles: two defects, the top of the pyramid and the edge of the hexagonal crystal). The profiles showed that the hillock was mainly growing during the experiment despite some regions (i.e. the end of section 3) showed dissolution. For a sake of clarity, all the six height channel topographies used for the measurement of the profiles are reported in the bottom part of the figure.

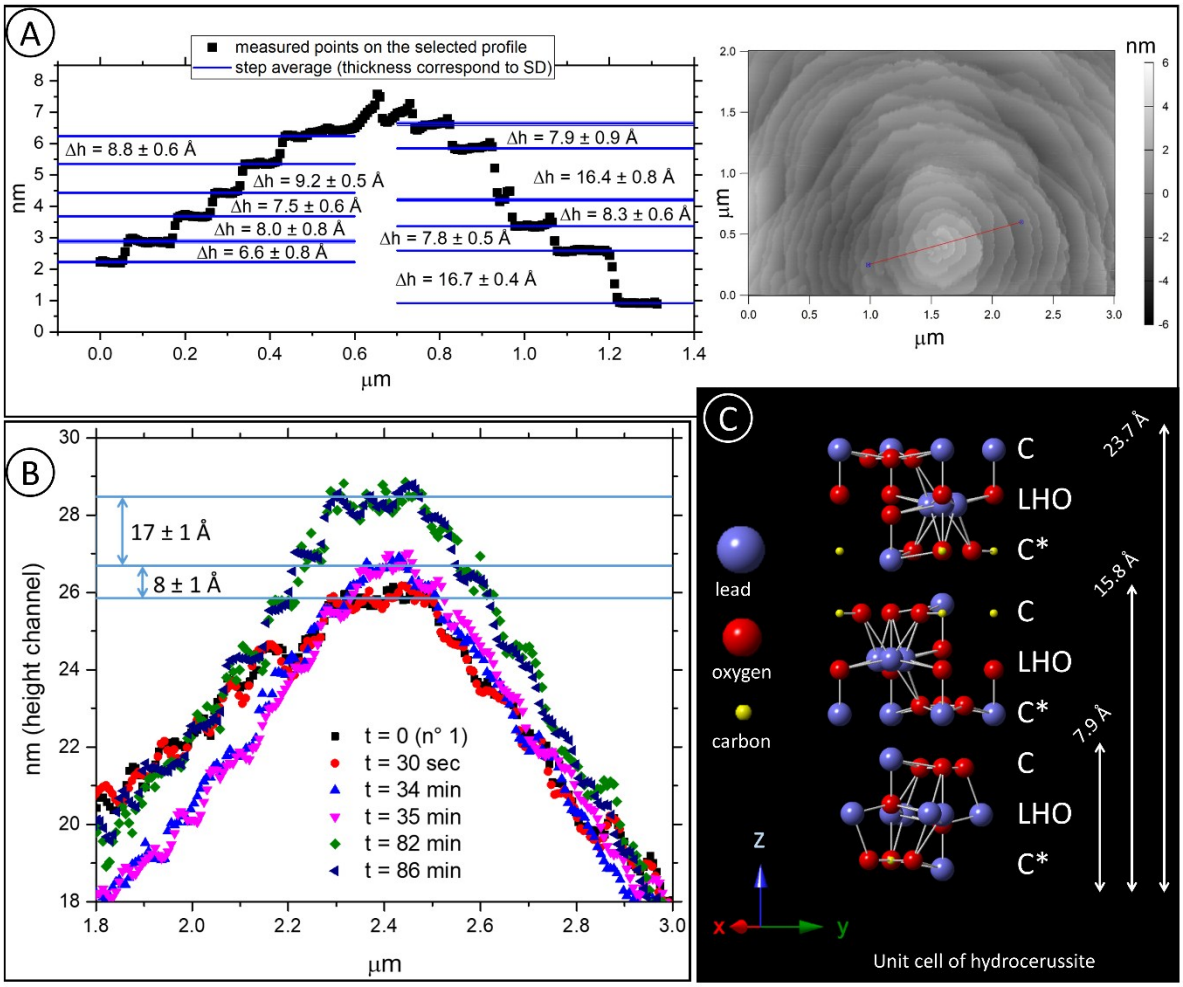

Figure S4. The top part of the image (A) show the results of an accurate steps measurement, the whole profile and the original images are also reported. Figure B corresponds to the top part of the profile n°1 presented in Figure S3, the evolution with time showed that the growth of HCER hillocks proceeded according to the layered structure of HCER. The unit cell of HCER (C) was reported for a comparison with the steps size measured by AFM.

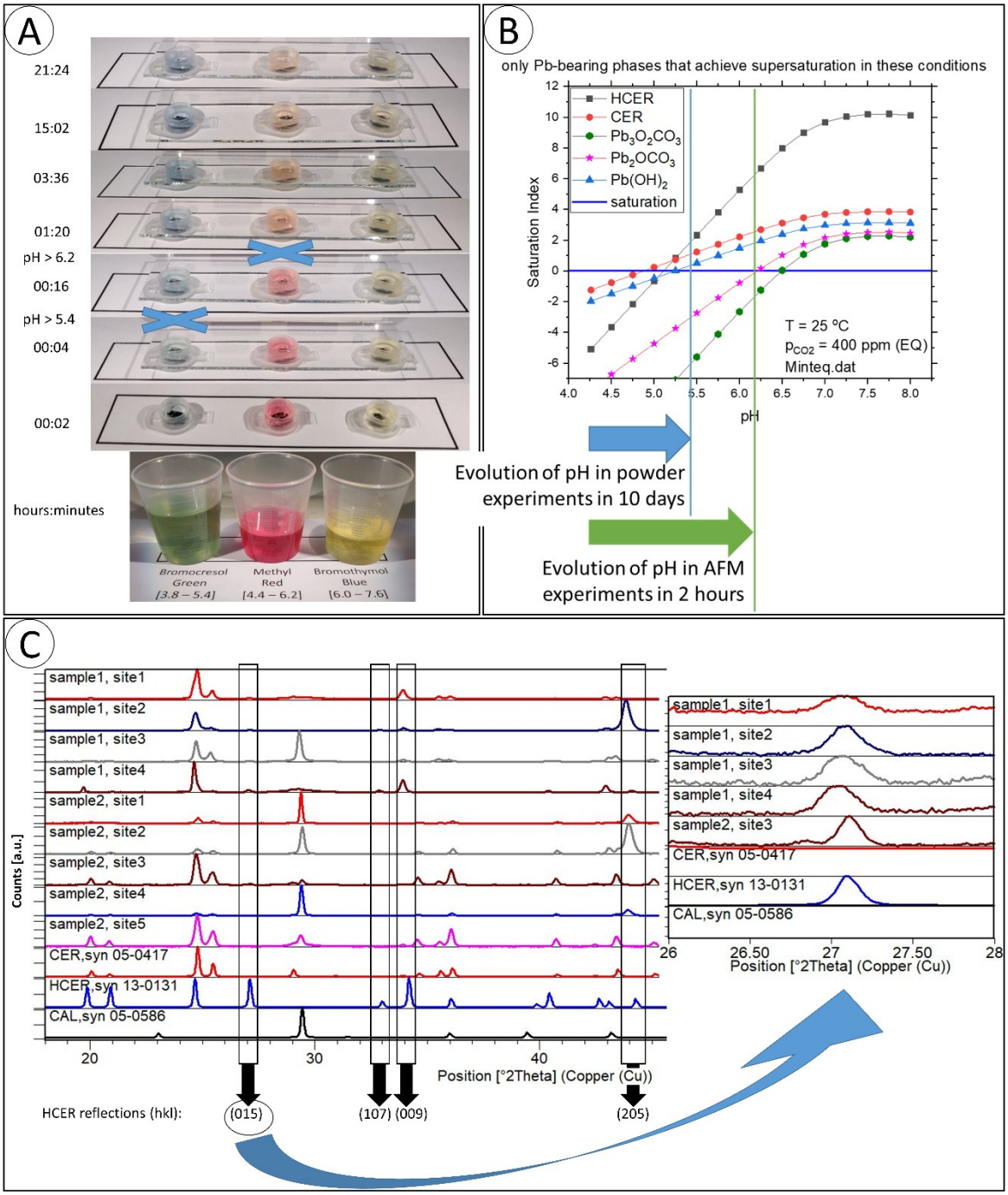

Figure S5. To understand the reasons behind the different behaviour between the powder experiments and the AFM experiments we combined ad hoc experiments and geochemical modelling. Figure A shows the evolution of pH during simulated AFM experiments (25 mg of a cleaved calcite crystal interacting with 0.23 mL of $Pb(NO_3)_2$ 0.01 M). Three pH indicators were used to monitor over time the alkalinisation of the solution due to CAL dissolution. The solid/liquid ratio used for AFM experiments resulted in higher pH: geochemical modelling (B) shows that such higher pH increases the thermodynamic driving force for precipitation of HCER much more than CER. X-ray diffraction (C) allowed observing the presence of reflections belonging to HCER, in particular the reflection at

27.2 °2θ was univocally attributed to HCER because CER and CAL have no reflections in this region.